

# A Three-Dimensional Architecture for a Parallel Processing Photosensing Array

Torbjorn Johansson, Masoud Abbasi, Robert J. Huber, *Member, IEEE*, and  
Richard A. Normann, *Member, IEEE*

**Abstract**—A three-dimensional architecture for a photosensing array has been developed. This silicon based architecture consists of a  $10 \times 10$  array of photosensors with  $80 \mu\text{m}$  diameter, through chip interconnects to the back side of a  $500 \mu\text{m}$  thick silicon wafer. Each photosensor consists of a  $300 \times 300 \mu\text{m}$  pn-junction photodiode. The following processes were used to create this photosensing architecture: 1) thermomigration of aluminum pads through an n-type silicon wafer; 2) creation of pn-junction photosensors on one side of the wafer; and 3) creation of aluminum pad ohmic contacts to the thermomigrated, through chip interconnects and the substrate on the back side of the wafer. The electrical and optical characteristics of the three-dimensional architecture indicates that it should be well suited as a photosensing framework around which a “silicon retina” could be built.

## INTRODUCTION

THE value of parallel processing has become increasingly apparent in the past years as the need for speed and more complex signal processing has increased. Parallel architectures are commonly used to increase the throughput of a circuit and the speed of computations. While most parallel processes implemented in hardware today use the well developed silicon planar technology, the complexity of the parallelism suggests that other technologies should be investigated. This has led to the development of three-dimensional architectures using amorphous silicon [1], [2], laser-recrystallization technology [3], and other architectures using interconnects both through and between silicon wafers [4].

A typical application of these three dimensional architectures is in data acquisition and signal processing from sensor arrays. Specifically, a two-dimensional array of sensors often requires multiplexing and/or signal processing circuitry which controls or selects the sensors and this circuitry can occupy a significant portion of the total surface area of the chip. If a three-dimensional architecture could be used to move the multiplexing and/or signal processing circuitry away from the sensors, the sensors could be made larger and sensor sensitivity could be increased

without decreasing the density of the sensor array. The development of a three-dimensional architecture could have greater impact on monolithic systems containing more complex multiplexing or signal processing circuitry, where the sensitivity could be substantially increased for the same density of sensors. One such three-dimensional architecture involves fabrication of the sensors on one surface of a silicon die and fabrication of the multiplexing and/or processing circuitry on the other side of the silicon die, with through-the-die interconnects connecting the sensors in the array with the processing circuitry.

Potential applications of three-dimensional data acquisition architectures are in the area of chemical or neurophysiological sensing where the sensors need to be both electrically and chemically isolated from the signal processing circuitry [3], [5]. An area where a three-dimensional architecture could have a substantial benefit is in “smart” photosensor arrays. A silicon retina, which includes extensive real-time signal processing, is an example of such a smart two dimensional photosensor array [6]–[8]. Extensive signal processing is necessary to mimic such functions as real-time spatial and temporal filtering of optical signals transduced by an array of high sensitivity photosensors. When additional retinal functions are implemented on these smart photosensing arrays, the required signal processing circuitry will be even more complex and occupy even more silicon area. If these functions are to be realized using a two-dimensional architecture, there will be an obvious tradeoff between photosensor sensitivity and the complex signal processing circuitry. Intelligent photosensor chips, using a two-dimensional architecture, have been developed to perform some of the processing on the sensor chip and some of the digital signal processing off chip [9]. A foveated, retina-like sensor using CCD technology has also been developed [10]. Both approaches are novel; however, as the functionality and parallelism is increased it can be advantageous to use a three dimensional architecture. The use of a three-dimensional architecture in the creation of a silicon retina, with sensors and signal processing circuitry fabricated on different planes in a laminar structure will eliminate the tradeoff between sensitivity and circuitry complexity, since the sensors and the signal processing circuitry will not compete for the same silicon surface area.

As a first step towards the creation of such a three-dimensional silicon retina, we have developed a three-di-

Manuscript received January 23, 1992; revised May 29, 1992. This work was supported by the William H. and Mattie Wattis Harris Foundation.

T. Johansson and R. J. Huber are with the Department of Electrical Engineering, The University of Utah, Salt Lake City, UT 84112.

M. Abbasi is with the Department of Mechanical Engineering, The University of Utah, Salt Lake City, UT 84112.

R. A. Normann is with the Department of Bioengineering, The University of Utah, Salt Lake City, UT 84112.

IEEE Log Number 9204054.

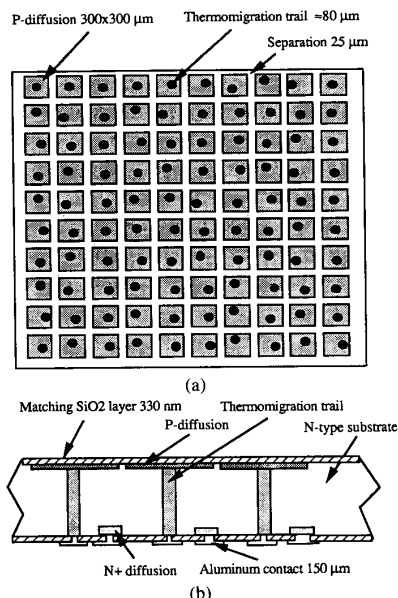


Fig. 1. A three-dimensional architecture for a parallel processing photosensing array. Top view (a) and side view (b).

mensional architecture for a parallel processing photosensing array, a  $10 \times 10$  array of photodiodes that fully occupy one surface of a silicon die. The output of each sensor is transmitted directly through the silicon die to its rear surface where a  $10 \times 10$  array of bonding pads has been formed. These bonding pads form the first generation output structure of the photosensing array. This paper describes how the architecture has been built and quantifies the characteristics of the system.

#### The Architecture of the Three-Dimensional Photosensing Array

The three-dimensional architecture for a parallel processing photosensing array consists of a  $10 \times 10$  array of photodiodes with interconnects through the wafer as shown in Fig. 1. The photodiodes are pn-junction silicon photodiodes formed by boron diffusion into the n-type silicon substrate. Each of the one hundred photodiodes has a dimension of  $300 \times 300 \mu\text{m}$  and is separated from its neighboring photodiodes by  $25 \mu\text{m}$ . The photosensing side with the pn-junctions is referred to as the "front side" of the die. The interconnects between the front side and the back side are thermomigrated trails made using the temperature gradient zone melting process (TGZMP) developed by Anthony and Cline [11]–[13]. This is a high-temperature process where a thermal gradient is produced across the silicon wafer, causing aluminum, deposited on the surface of the wafer, to migrate through the wafer as an Al-Si alloy droplet. As the droplet moves through the wafer, it leaves behind a highly conductive trail of p-doped silicon. Each thermomigration trail has an average diameter of  $80 \mu\text{m}$ . Aluminum square pads,  $150 \mu\text{m}$  on a side, make contact to the p-doped trails which emerge

from the silicon die. The side of the wafer containing the aluminum contact pad is referred to as the "back side" of the wafer. Thus, the highly conductive p-type thermomigrated trails connect the photodiodes to the aluminum contacts on the back side of the die. An additional set of aluminum pads on the back side of the wafer make a low resistance ohmic contact to the  $n^+$ -doped silicon substrate.

Since this is a double-sided semiconductor process, cleanliness of both the front and back side of the wafer was essential. Single-sided photolithography does not protect the back side of the wafer while processing the front side and vice versa. Therefore, a "double-sided photolithographic process" was developed to protect the side of the die that was not being processed.

#### METHODS OF PREPARATION

##### Sample Preparation

Single-crystal, 3 in diam  $\langle 100 \rangle$  silicon wafers were used for the fabrication of the three-dimensional photosensing arrays. These were  $10 \Omega\text{-cm}$  n-type phosphorus doped wafers and were  $1900 \mu\text{m}$  thick with only one side polished. After a hydrogen peroxide based wafer cleaning procedure [14], approximately  $3 \mu\text{m}$  of aluminum was evaporated onto the silicon wafer. Positive photolithography was used to form 24 arrays, each of which contained a matrix of  $10 \times 10$  aluminum squares. The aluminum squares were  $100 \mu\text{m}$  on a side and were placed with their centers  $325 \mu\text{m}$  apart. A dicing saw with a  $50 \mu\text{m}$  wide blade was then used to scribe indexing marks into the silicon surface for subsequent aligning of the masks used during the double-sided silicon photolithographic processes.

##### Thermomigration

The temperature gradient zone melting process (TGZMP) was used to form the interconnects between the front and back sides of the wafer. The TGZMP is a process in which a liquid zone in the form of a sheet, rod or droplet migrates through a solid under the driving force of a temperature gradient. Since aluminum is a p-type dopant, the remaining trails are highly conductive  $p^+$  silicon. The TGZMP apparatus and procedure we used to create these structures is described elsewhere [15].

##### Wafer Polishing

After the thermomigration, the 3 in wafer was cut on a dicing saw into six squares with dimensions of approximately  $20 \times 20 \text{ mm}$ . Each of the six silicon wafers contained four  $10 \times 10$  arrays of aluminum trails. The thermomigration process damaged both sides of the wafer. At the entry side of the silicon dice, aluminum oxide and residues of the aluminum were left not only above the surface but also below the surface and therefore this surface had to be repolished. The exit sides of the aluminum also tended to "smear out" considerably after it com-

pletely migrated through the wafer. Thus, the dice were ground down from the exit side to a thickness of approximately  $500\ \mu\text{m}$  before they were polished. Both sides of the wafers were then polished removing approximately  $30\ \mu\text{m}$  on each side, starting with a  $30\ \mu\text{m}$  diamond compound on a polishing wheel and continuing with compound sizes of 15, 6, 1, and  $\frac{1}{4}\ \mu\text{m}$ . After the polishing, the silicon dice had a double sided polish and contained a matrix of p-trails through the n-type substrate. Before subsequent oxidation processes and the diffusion processes the wafers were put through a series of cleaning steps a second time to remove any metals, organic compounds or other contaminants.

### Photodiode Processing

The  $300 \times 300\ \mu\text{m}$  p-doped regions on the front side of the wafer were formed next. A layer of  $\text{SiO}_2$  was thermally grown at  $1000^\circ\text{C}$  on the silicon wafers first in a dry oxygen atmosphere for 10 min followed by a wet oxidation for 70 min. This yielded a  $380\ \text{nm}$  layer of  $\text{SiO}_2$ .

Since the creation of the photosensor array is a two-sided process, a double-sided photolithographic process was developed. Cleanliness of both the front and back sides was essential during the double-sided photolithographic processes. In order to protect the side of the silicon wafer that was not being processed during the photolithography, a special holder, machined from polyethylene, kept one side of the wafer clean except for the very outer edges. The photoresist was spun on and cured in an oven at  $130^\circ\text{C}$  for 30 min. This photoresist protected the back side of the silicon die from scratches and contaminants during the photolithographic process. The holder was used one more time when photoresist was spun on the other side of the wafer. The silicon wafer was then processed with conventional single sided photolithographic steps.

After the photolithography, the silicon wafer was coated with a layer of spin-on dopant (boron atom concentration of  $10^{21}\ \text{cm}^{-3}$ ) on the front side of the wafer to form the photodiodes. This was given a drive-in treatment at  $992^\circ\text{C}$  for 15 min to form pn-junction photodiodes with a junction depth calculated to be  $0.25\ \mu\text{m}$ . The  $300 \times 300\ \mu\text{m}$  square boron diffused p-region areas were aligned over the p-type thermomigration trails to ensure that the trails contacted the p-regions. The doped spin-on glass was removed from the die and another silicon oxidation was performed for the next process step. The same steps in the photolithographic process were applied as before, but now the photosensing side of the wafer was protected with a layer of hard-baked photoresist. To make low resistance ohmic contacts to selected sides on the silicon substrate, a spin-on phosphorus dopant glass was used as a source to create heavily doped  $\text{n}^+$  contact regions. The spin on dopant was given a drive-in treatment at  $1000^\circ\text{C}$  for 15 min to form a high-low doping transition at a depth calculated to be  $0.8\ \mu\text{m}$ . All the  $\text{SiO}_2$  was removed and a new layer of  $\text{SiO}_2$  was thermally grown at  $1000^\circ\text{C}$  first in

a dry oxygen atmosphere for 5 min followed by a wet oxidation for 55 min, resulting in a  $330\ \text{nm}$  layer of  $\text{SiO}_2$ . This was done to produce a second order,  $\frac{1}{4}$ -wave matching layer for the photons striking the photosensing side of the wafer and as a masking layer on the opposite side of the wafer. Again, "double side" photolithography was performed to etch the holes in the  $\text{SiO}_2$  for contacts to the p-trails and to the phosphorus doped substrate. A  $8000\ \text{\AA}$  layer of aluminum was evaporated onto the wafer and patterned to have square,  $150\ \mu\text{m}$  contact pads. Aluminum alloy was formed at  $425^\circ\text{C}$  for 30 min in hydrogen and nitrogen ambient.

## EXPERIMENTAL RESULTS

### Yield

Out of the sixteen  $10 \times 10$  arrays of photosensors that survived the manufacturing processes, 98% of the thermomigration trails made contact to the p-diffusion regions. Two percent of the thermomigration trails failed to contact the photosensor p-region due to the random walk nature of the TGZMP process. In this particular application, random walk, a well-known phenomena in the thermomigration process [15], [16] was not a major concern as long as the trails migrated sideways less than  $150\ \mu\text{m}$ . If the TGZMP trail deviated more than  $150\ \mu\text{m}$  from the center, it made contact to a neighboring p-region. It is also possible for the trail to make contact to two neighboring p-diffusion regions if the center of the trail exits the silicon wafer between two p-diffusion regions and makes contact to both regions. Thus, the random walk had to be limited to a deviation of  $150\ \mu\text{m}$  from the center to achieve a 100% yield. The random walk of the trails can be seen in Fig. 2. Detailed results of the TGZMP process are presented in a separate paper [15].

### PN-Junction Characteristics

The pn-junction characteristics depend both upon the quality of the pn-junction of the p-doped TGZMP trail and the spin-on boron dopant. Approximately half of the total pn-junction area was formed by the thermomigration process and half by the diffusion and drive-in treatment of the boron-dopant spin-on glass.

The current-voltage characteristics of these junctions were measured with an HP4145 analyzer. The forward biased characteristics for currents ranging from 100 pA to 1 mA are shown in Fig. 3 and show an approximately logarithmic dependence of current upon forward bias voltages over about 5 log units. Deviations from the log is due to a series resistance or a high level injection of carriers.

The current in the pn-junction for different reverse bias voltages, shown in Fig. 4, is a generation current in the pn-junction which increases as the voltage across the reverse biased junction increases. The dark current increases linearity with the reverse biased voltage across the junction from 0 pA (with zero bias) to 1.9 nA (at 5 V) due to the increase in generation current. Since the di-

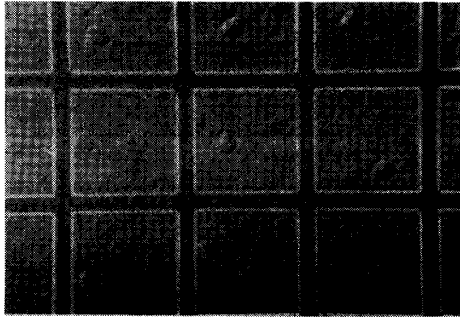


Fig. 2. Nine pixels out of the  $10 \times 10$  array of photosensors. The circular objects are the thermomigrated trails that make contact with the p-diffusion photosensor regions. The random walk of the thermomigration trails can be observed. Each photodiode is  $300 \mu\text{m}$  on a side.

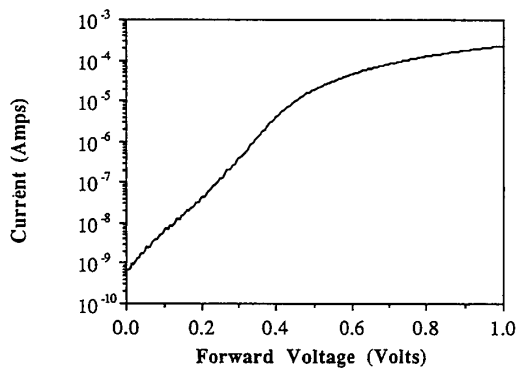


Fig. 3. Forward bias characteristics of a typical pn-junction at different voltages. The forward bias characteristics show an approximately logarithmic relation between current and forward bias voltages across the pn-junction over about 5 log units.

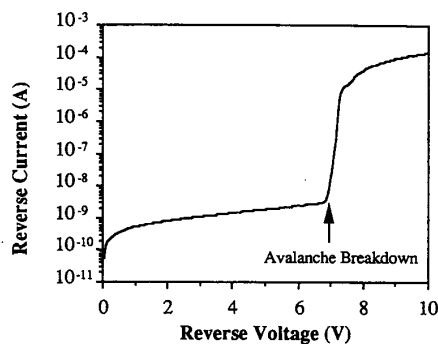


Fig. 4. Reverse bias characteristics of a typical pn-junction. The reverse bias characteristics show a linear relation between current and reverse bias voltage across the pn-junction over about 7 V.

ameter of the circular shaped thermomigration trail varies at different depths in the silicon die, only an estimate of the leakage current per  $\mu\text{m}^2$  can be made. Calculations based on average thermomigration trail diameter of  $80 \mu\text{m}$  results in a leakage current of  $1.1 \times 10^{-6} \text{ A/cm}^2$  at 5 V. The relatively high leakage current and ideality factor ( $n = 1.65$ , Fig. 3) is due to the high recombination rate in the depletion region around the thermomigrated column.

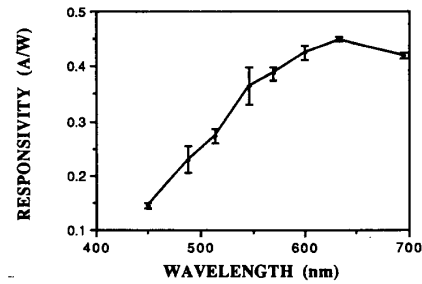


Fig. 5. Spectral sensitivity of the photodiodes in the visual spectrum. The photosensors have a peak responsivity of  $0.45 \text{ A/W}$  at approximately  $650 \text{ nm}$ . The error bars show the standard deviation of the measurements in ten photodiodes.

The reverse breakdown voltage of the pn-junctions varied from 7 to 10 V with an average break down voltage of 8.5 V. The low avalanche breakdown voltage is due to the very shallow p-diffused photosensor region.

#### Optical Characteristics

The optical characteristics were determined over the visual spectrum with eight different interference filters (Edmond Scientific). The photodiode current was measured using a current-to-voltage amplifier. The responsivity of the zero biased photosensors in the visual spectrum is shown in Fig. 5. The responsivity reached a peak of  $0.45 \text{ A/W}$  at approximately  $650 \text{ nm}$ . The responsivity of a photodiode without a thermomigrated trail would be higher because of a larger depletion volume. The peaking of responsivity at this low wavelength is mainly due to the shallow depth of the pn-junction and to the added  $330 \text{ nm}$  thick layer of  $\text{SiO}_2$ . The  $\text{SiO}_2$  layer on the photosensors acts like an antireflection coating to improve the performance of the photodiodes. The  $\frac{1}{4}$  wave, second harmonic matching layer of  $\text{SiO}_2$  increases the sensitivity in the visual spectrum with an anti-reflection maximum at  $610 \text{ nm}$ .

The responsivity is expected to increase a few percent with the photodiode back biased, since the width of the pn-junction depletion region increases. The reverse biased peak responsivity was  $0.49 \text{ A/W}$  at reverse biased voltage of 5 V compared to  $0.45 \text{ A/W}$  for a zero biased junction, a 9% increase in responsivity for a reverse biased pn-junction.

#### Blooming

Photons absorbed in one sensor can inject current into an adjacent sensor. This undesired current injection is known as blooming and is a potential problem in many photosensor arrays. A potential barrier in the form of an  $n^+$  doping region between the neighboring sensors is often used to minimize blooming.

Blooming was measured by connecting two adjacent photodiodes as a pnp transistor and sending current through the base emitter junction. A transistor gain (beta) of  $1/10\,000$  was measured with an  $I-V$  curve tracer. This

indicates that the photosensors are disconnected due to the large distance between them and/or the short carrier lifetime in the n-type substrate. Photodiodes not adjacent to the sites of current injection showed no measurable blooming (a beta of less than  $10^{-6}$ ).

#### DISCUSSION

We have shown that a three dimensional architecture of photodiodes and cross wafer interconnects results in a parallel processing photosensing array of relatively high quality. Before this architecture can be used in a silicon retina application, three important issues need further consideration. The first is the reduction of the dimensions of the photosensors. There are three major factors that limit the dimensions of the structures used in this device; the size of through chip interconnects which can be thermomigrated through the wafer, the warping of the wafer when the thermomigration occurs at high temperatures, and the random walk of the thermomigration columns. Thermomigration columns as small as  $100\ \mu\text{m}$  have been reported [3] and we have occasionally thermomigrated columns as small as  $15\ \mu\text{m}$  through the wafer. However, this was achieved at such a high temperature and with such an uneven temperature distribution across the wafer, that a warping of the silicon wafer was often produced. Such warped wafers can not be used for further processing. The problem of warping of the silicon wafer and the thermomigration process is discussed further in a separate paper [15]. The random walk which occurs in the thermomigration process is a well known phenomena [16] and Anthony and Cline have reported ways to reduce the problem. However, because of the relatively large size of the photodiode "targets" used in this array, random walk was not a significant problem. Smaller photodiode targets will require greater control over the random walk problem.

The second important issue that must be addressed is the complexity of the photosensor signal processing circuitry on the back side of the silicon die. The possibility of putting multiplexing circuitry and/or signal processing circuitry on the back side of the sensor array is a question of processing techniques. The cleanliness of both surfaces while processing will be essential. Basically, the same process techniques described herein can be used to fabricate transistors on the back side; however, the polishing of the wafer surfaces has to be improved with a chemical polishing step to achieve high quality transistors. Instead of fabricating circuitry on the back side of the silicon die, another die containing signal processing circuitry can be mounted using solder bump technology to the three dimensional architecture photosensing die, Fig. 6 [17]. This approach may be more cost and process effective.

Third, the benefits accruing from a three dimensional structure may not justify the added manufacturing complexity. The increase in performance associated with the use of the three dimensional architecture will vary with the size and design of the signal processing circuitry and the size of the photosensors. Three main design criteria

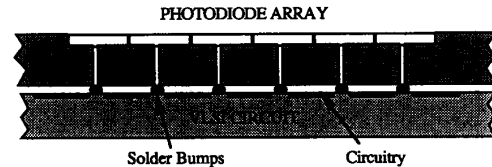


Fig. 6. The three-dimensional architecture photosensing die and a silicon die containing signal processing circuitry are connected using solder bump technology.

have to be considered; signal-to-noise ratio ( $S/N$ ), sensitivity and density of sensors.

The signal-to-noise ratio is degraded by going from a 2-D to the three dimensional architecture described in the paper because of the extra dark current associated with the thermomigration trails to the back side of the silicon die. However, the  $S/N$  degradation is minimized as the size of the thermomigration trails are reduced. If the increase in dark current due to the thermomigration trails does not limit or significantly degrade the performance of the signal processing circuitry, the performance of the three dimensional parallel architecture can be beneficial.

On the other hand, the sensitivity of the sensor can be improved with the three-dimensional architecture because the signal processing circuitry can be removed from the plane of the sensors. This allows an enlargement of the photosensor area and increases the number of photons which can be absorbed by the photosensors. The increase in sensitivity which can be realized by the three-dimensional architecture is therefore a function of the ratio of photosensitive area and signal processing circuitry area. The more complex the signal processing circuitry, the more the sensitivity can be improved by moving the circuitry to the back side of the array.

The density of the array of sensors can also be improved with a three-dimensional architecture. The size of the thermomigration trail and the size of the circuitry sets limits on the improvement of the density of the sensor array. Since the size of the thermomigration trails can be relatively large in comparison to the size of the pixels, the density of the sensors is in many cases limited by the size of the thermomigration trail. The other limitation to the density of the pixels is the size of the signal processing circuitry associated with each pixel. For large numbers of photosensors, the silicon area of each photosensor should be equal to the area of the signal processing circuitry on the back side of the array. Thus, the size of this circuitry will generally set a limit on the photosensor density.

Our main interest in developing the three-dimensional photosensing array described herein is that it will provide a functional foundation for a silicon retina. Different signal processing circuits have already been developed to mimic the functions in the retina. Important preprocessing functions produced by the human retina are spatial and temporal filtering as well as gain control by the photoreceptors themselves. First, generation silicon retinas contained analog signal processing circuitry with most of the silicon real estate occupied by the processing circuitry [8].

Later versions have improved the ratio of photosensitive area to circuit area [6], but as more of the functionality of the human retina is implemented in the signal processing circuitry, the ratio of sensor area to circuitry area, and photosensitivity must decrease [7]. A three-dimensional silicon retina with sensors and signal processing circuitry fabricated on different planes in a laminar structure will eliminate this tradeoff, since the sensors and the signal processing circuitry will not compete for the same real estate. Thus, such a three-dimensional silicon architecture with its retinal signal processing will not only mimic some of the functions of the human retina but it will achieve this function using a laminar architecture similar to that of the retina.

#### ACKNOWLEDGMENT

The authors wish to thank D. Petelenz for many useful discussions and L. Sadwick for his help with some of the measurements.

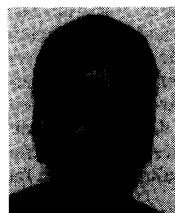
#### REFERENCES

- [1] H. Ohshima and S. Morozumi, "Future trends for TFT integrated circuits on glass substrates," *IEEE Internat. Electron Dev. Meet.*, pp. 157-160, 1989.
- [2] W. Sah, S. Lee, and J. Chen, "Amorphous silicon edge detector for application to electronic eyes," *IEEE Internat. Electron Dev. Meet.*, pp. 515-518, 1989.
- [3] S. J. Kim, M. Kim, and W. J. Heetderks, "Laser-induced fabrication of a transubstrate microelectrode array and its neurophysiological performance," *IEEE Trans. Biomed. Eng.*, vol. BME-32, pp. 497-502, July 1985.
- [4] M. J. Little, R. D. Etchells, J. Grinberg, S. P. Laub, J. G. Nash, and M. W. Yung, "3-D Computer," *IEEE Internat. Conf. Wafer Scale Integration*, pp. 55-64, 1989.
- [5] C. Wen, T. C. Chen, and J. N. Zemel, "Gate-controlled diodes for ionic concentration measurement," *IEEE Trans. Elec. Dev.*, vol. 6, pp. 1945-1951, Dec. 1979.
- [6] K. A. Boahen and A. G. Andreou, "A contrast sensitive silicon retina with reciprocal synapses," *IEEE Proc. Neural Information Proc. Syst.*, 1991.
- [7] M. A. Mahowald, "Silicon retina with adaptive photoreceptors," *SPIE Internat. Symp. Op. Eng. Photonics in Aerospace Sensing*, pp. 1473-1504, 1991.
- [8] C. A. Mead, *Analog VLSI and Neural Systems*. Reading, MA: Addison-Wesley, 1989.
- [9] R. Ginosar and Y. Zeevi, "Adaptive sensitivity/intelligent scan image processor," *SPIE*, 1988.
- [10] J. Van der Spiegel *et al.*, *A Foveated Retina-Like Sensor Using CCD Technology*. Boston, MA: Kluwer, 1989, ch. 8, pp. 189-210.
- [11] T. R. Anthony and H. E. Cline, "Stress generated by the thermomigration of liquid inclusions in silicon," *J. Appl. Phys.*, vol. 49, pp. 5774-5782, Dec. 1978.
- [12] H. E. Cline and T. R. Anthony, "High-speed droplet migration in silicon," *J. Appl. Phys.*, vol. 47, no. 6, pp. 2325-2331, 1976.
- [13] —, "Nonequilibrium morphology of liquid inclusions migrating in solids," *J. Appl. Phys.*, vol. 48, no. 12, pp. 5096-5104, 1977.
- [14] W. Kern and D. A. Puotinen, "Cleaning solutions based on hydrogen peroxide for use in silicon semiconductor technology," *RCA Rev.*, pp. 187-206, June 1970.
- [15] M. Abbasi, T. Johansson, and R. A. Normann, "Silicon-carbide-enhanced thermomigration," *J. Appl. Phys.*, in press.
- [16] T. R. Anthony and H. E. Cline, "Random walk of liquid droplets migrating in silicon," *J. Appl. Phys.*, vol. 47, pp. 2316-2324, 1976.
- [17] L. F. Miller, "Controlled collapse reflow chip joining," *IBM J. Res. Develop.*, May 1969.



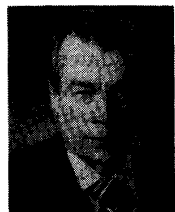
**Torbjorn Johansson** received the B.S. degree in electrical engineering magna cum laude from the University of Utah, Salt Lake City, in 1988. He was selected the 1988 male student athlete at the university as a member of the university swimming team.

He is currently pursuing the Ph.D. degree in electrical engineering from the University of Utah, Salt Lake City. His research centers on the creation of a three dimensional silicon retina suitable for use in an artificial vision prosthesis. Other research interests are analog VLSI and architectures for hardware implementation of neural networks.



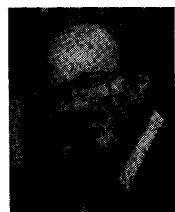
**Masoud Abbasi** received the B.S. degree in chemical engineering in 1989 and the M.S. degree in mechanical engineering in 1992 from the University of Utah, Salt Lake City.

He is currently pursuing the Ph.D. degree in mechanical engineering from the University of Utah, Salt Lake City. His current research involves the thermoelectric properties of semiconductors and thermoelectric generation for heating and refrigeration applications. His research interests include fluid mechanics, and heat transfer and diffusion of impurities in semiconductors.



**Robert J. Huber** (M'69) received the B.S. and Ph.D. degrees in physics from the University of Utah, Salt Lake City.

After graduating he worked with nuclear reactor physics at Argonne National Laboratory. He joined the Microelectronic Division of General Instrument Corp. in 1966 and worked on MOS device physics. From 1971 through 1977 he was with the University of Utah Institute for Biomedical Engineering working on the neuroprosthesis program. He has been a faculty member of the Department of Electrical Engineering, University of Utah since 1977. His current research interests are silicon device physics and solid state sensors and actuators.



**Richard A. Normann** (M'88) received the Bachelor's, Masters, and Doctor of Philosophy degree from the University of California, Berkeley.

He joined the staff of the National Institute of Health in 1974 and remained there until 1979 when he moved to the Department of Bioengineering. He also holds Research and Adjunct Professorships in the Departments of Ophthalmology and Physiology in the School of Medicine at the University of Utah. His research interests are: information processing in the vertebrate retina and neuroprosthetics (creating interfaces to the nervous system).